

COMPLETE WEAK-SCALE THRESHOLD CORRECTIONS IN THE MINIMAL SUPERSYMMETRIC STANDARD MODEL

J. BAGGER, K. MATCHEV AND D. PIERCE

*Department of Physics and Astronomy
The Johns Hopkins University
Baltimore, MD 21218, USA*

ABSTRACT

We compute the full set of weak-scale gauge and Yukawa threshold corrections in the minimal supersymmetric standard model, and use them to study the effects of the supersymmetric particle spectrum on gauge and Yukawa coupling unification.

1. Introduction

The idea of supersymmetric unification has received a significant boost from the recent observation that the gauge couplings unify in the minimal supersymmetric standard model.¹ Indeed, this observation has given great impetus to the search for supersymmetric particles at present and future accelerators. In this talk we will assume that supersymmetry has been found, and ask what the supersymmetric particle spectrum can tell us about unification-scale physics.

To lowest order, the answer is not much, because the one-loop renormalization group equations (RGE's) do not depend on the physics of the unification scale. To second order, the story is different. This is because the two-loop RGE's must be used in conjunction with the one-loop threshold corrections. The threshold conditions depend on the weak-scale supersymmetric spectrum *and* on the unknown unification-scale physics. Therefore to second order, the superparticle spectrum is correlated with the physics of the unification scale.

In this talk we will report on results of a complete next-to-leading-order analysis of supersymmetric unification. Our results are based on the full set of two-loop supersymmetric renormalization group equations, together with the complete one-loop threshold conditions, including finite parts. We use a two-sided differential equation solver which allows us to impose boundary conditions at the weak scale, M_Z , and at the unification scale, M_{GUT} .

At the weak scale, we specify the \overline{DR} gauge couplings $\hat{g}_1(M_Z)$ and $\hat{g}_2(M_Z)$, and the \overline{DR} vev \hat{v} , which we extract from the Fermi constant, G_F , the Z -boson mass, M_Z , and the electromagnetic coupling α_{EM} . We also specify the top and tau \overline{DR} Yukawa couplings $\hat{\lambda}_t(M_Z)$ and $\hat{\lambda}_\tau(M_Z)$, which we compute from $\tan\beta \equiv \tan\hat{\beta} = \hat{v}_2/\hat{v}_1$ and the top and tau pole masses, m_t and m_τ .

We define M_{GUT} to be the scale where $\hat{g}_1(M_{\text{GUT}}) = \hat{g}_2(M_{\text{GUT}})$. At M_{GUT} we specify the \overline{DR} supersymmetric parameters $M_{1/2} \equiv \hat{M}_{1/2}(M_{\text{GUT}})$, $M_0 \equiv \hat{M}_0(M_{\text{GUT}})$,

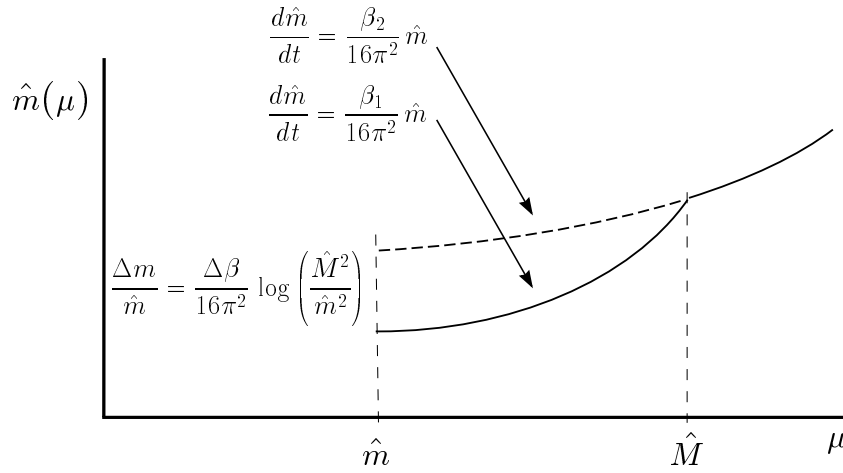


Fig. 1. The \overline{DR} mass $\hat{m}(\mu)$ vs. the \overline{DR} scale $\mu = e^t$.

and $A_0 \equiv \hat{A}_0(M_{\text{GUT}})$. We also define the \overline{DR} strong coupling $\hat{g}_3(M_{\text{GUT}})$ by the unification condition

$$\hat{g}_3(M_{\text{GUT}}) = \hat{g}_1(M_{\text{GUT}})(1 + \epsilon_g) , \quad (1)$$

where ϵ_g parametrizes the gauge-coupling threshold correction at the unification scale. In a similar way, we impose bottom-tau unification and define the bottom-quark \overline{DR} Yukawa coupling to be

$$\hat{\lambda}_b(M_{\text{GUT}}) = \hat{\lambda}_\tau(M_{\text{GUT}})(1 + \epsilon_b) , \quad (2)$$

where ϵ_b parametrizes the unification-scale Yukawa coupling threshold correction.

We solve the supersymmetric renormalization group equations self-consistently, subject to the boundary conditions at M_Z and M_{GUT} . In this way we find a prediction for the \overline{DR} couplings $\hat{g}_3(M_Z)$ and $\hat{\lambda}_b(M_Z)$. We then apply the weak-scale threshold corrections to determine the \overline{MS} strong coupling, $\alpha_s(M_Z)$, the bottom-quark pole mass, m_b , and the full supersymmetric particle spectrum. Our results allow us to correlate the unification-scale thresholds ϵ_g and ϵ_b with m_b , $\alpha_s(M_Z)$ and the superparticle spectrum.

2. Threshold Corrections

2.1. The Match-and-Run Procedure

To study unification-scale physics, it is important to use the correct weak-scale threshold corrections. Typically, these corrections are computed using the so-called match-and-run technique, which is based on the successive decoupling of particles at the scale of their masses. As an example of this technique, let us consider a running \overline{DR} mass \hat{m} , whose full β -function depends on all the particles in the supersymmetric standard model. For large renormalization scales μ , \hat{m} evolves according to its complete supersymmetric RGE.

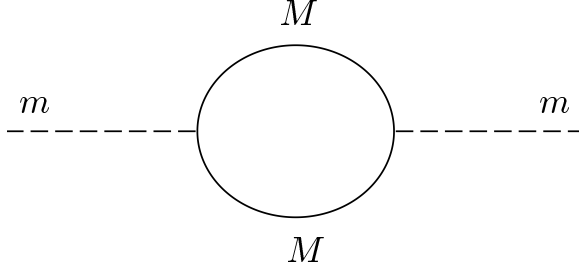


Fig. 2. The one-loop diagram that yields the threshold correction for a particle of mass m from a particle of mass M .

Let us now run \hat{m} towards the weak scale, M_Z . Along the way, we eventually encounter the scale of the squark masses. According to the match-and-run procedure, we must stop the evolution and construct a new effective theory in which the squarks are integrated out. We must then continue the evolution, using the new β -function, without the squark contribution, subject to the matching condition $\hat{m}(m_{sq}^-) = \hat{m}(m_{sq}^+)$. We repeat this procedure at each new threshold, finally stopping at the scale $\mu = \hat{m}(\mu)$. The quantity $\hat{m}(\hat{m})$ is the match-and-run approximation to the physical pole mass.

To test this procedure, let us compute the threshold correction to a particle of mass \hat{m} from a particle of mass M , with $M > m$. According to the match-and-run procedure, the decoupling of the heavy particle gives the correction

$$\frac{\Delta m}{\hat{m}} = \frac{\Delta\beta}{16\pi^2} \log\left(\frac{\hat{M}^2}{\hat{m}^2}\right), \quad (3)$$

as shown in Figure 1. In this expression, $\Delta\beta$ is the difference of the β -functions, before and after decoupling.

The exact one-loop result can be found by computing the diagram of Figure 2. It is given by

$$\frac{\Delta m}{\hat{m}} = \frac{\Delta\beta}{16\pi^2} \int_0^1 dx \log\left(\frac{|M^2 - x(1-x)m^2|}{\mu^2}\right). \quad (4)$$

For $\mu = m$, this reduces to

$$\frac{\Delta m}{\hat{m}} = \frac{\Delta\beta}{16\pi^2} \left[\log\left(\frac{M^2}{m^2}\right) + \text{finite} \right], \quad (5)$$

where the finite contribution does not contain any logarithms.

These results indicate that the match-and-run procedure gives a good approximation to the pole mass when $\hat{M} \gg \hat{m}$. In this case the large logarithm, proportional to $\log(\hat{M}^2/\hat{m}^2)$, dominates the threshold correction.

When $\hat{m} \simeq \hat{M}$, however, the finite term is typically as large as the logarithm. The finite correction is completely missed by the match-and-run procedure. In supersymmetric unified models with universal boundary conditions, it is quite possible

for all the supersymmetric masses to be near M_Z , in which case the match-and-run procedure gives an error of $\mathcal{O}(1)$.

2.2. Gauge Coupling Thresholds

It is important to use the correct weak-scale threshold corrections because supersymmetric unification depends sensitively on the weak-scale boundary conditions. This can be easily understood from the one-loop renormalization group equations for the gauge couplings. Assuming unification, the RGE's imply

$$\frac{\beta_2 - \beta_3}{\hat{g}_1^2(\mu)} + \frac{\beta_3 - \beta_1}{\hat{g}_2^2(\mu)} + \frac{\beta_1 - \beta_2}{\hat{g}_3^2(\mu)} = 0 , \quad (6)$$

at any scale μ , where the β_i are the one-loop β -functions for the running gauge couplings. Solving for $\alpha_s(M_Z)$ and varying the inputs $\hat{g}_1(M_Z)$ and $\hat{g}_2(M_Z)$, one finds

$$\frac{\delta\alpha_s}{\alpha_s(M_Z)} \simeq -10.6 \frac{\delta\hat{g}_1}{\hat{g}_1(M_Z)} + 12.2 \frac{\delta\hat{g}_2}{\hat{g}_2(M_Z)} . \quad (7)$$

This implies that an error in the determination of $\hat{g}_1(M_Z)$ or $\hat{g}_2(M_Z)$ of 1% percent can lead to an error in the evaluation of $\alpha_s(M_Z)$ of more than 10%.

The fact the RGE's can naturally amplify small errors means that one must determine the weak-scale threshold corrections to complete one-loop accuracy. Therefore, in our analysis, we compute $\hat{g}_1(M_Z)$ and $\hat{g}_2(M_Z)$ directly from the Fermi constant, $G_F = 1.16639 \times 10^{-5} \text{ GeV}^{-2}$, the Z -boson mass $M_Z = 91.187 \text{ GeV}$, the electromagnetic coupling $\alpha_{\text{EM}} = 1/137.036$, the top-quark mass m_t , and the parameters that describe the supersymmetric model. We include logarithmic and finite contributions, so our results are more accurate than those based on the match-and-run procedure. Note that we do not use the best-fit value of the standard-model weak mixing angle, $\sin^2 \theta_{\text{SM}}$. This is because the standard-model value of $\sin^2 \theta_{\text{SM}}$, extracted from a combined fit to the data, cannot be used in a supersymmetric analysis when finite corrections are important. (See also [2]. We did not include the complete gauge coupling thresholds in the preliminary results presented at the conference.)

We start our analysis by computing the electromagnetic coupling $\hat{\alpha}$ and the supersymmetric weak mixing angle \hat{s}^2 in the \overline{DR} renormalization scheme,

$$\hat{\alpha} = \frac{\alpha_{\text{EM}}}{1 - \Delta\hat{\alpha}} , \quad \hat{s}^2 \hat{c}^2 = \frac{\pi\alpha_{\text{EM}}}{\sqrt{2}G_F M_Z^2 (1 - \Delta\hat{r})} , \quad (8)$$

where $\hat{c}^2 = 1 - \hat{s}^2$,

$$\begin{aligned} \Delta\hat{\alpha} = & 0.0658 \pm 0.0007 - \frac{\alpha_{\text{EM}}}{2\pi} \left\{ -\frac{7}{4} \log\left(\frac{M_W}{M_Z}\right) + \frac{16}{9} \log\left(\frac{m_t}{M_Z}\right) + \frac{1}{3} \log\left(\frac{m_{H^+}}{M_Z}\right) \right. \\ & \left. + \sum_{i=1}^6 \frac{4}{9} \log\left(\frac{m_{\tilde{u}_i}}{M_Z}\right) + \sum_{i=1}^6 \frac{1}{9} \log\left(\frac{m_{\tilde{d}_i}}{M_Z}\right) + \sum_{i=1}^3 \frac{1}{3} \log\left(\frac{m_{\tilde{e}_i}}{M_Z}\right) + \sum_{i=1}^2 \frac{4}{3} \log\left(\frac{m_{\chi_i^+}}{M_Z}\right) \right\} , \end{aligned} \quad (9)$$

and³

$$\Delta\hat{r} = \Delta\hat{\alpha} + \frac{\hat{\Pi}_W(0)}{M_W^2} - \frac{\hat{\Pi}_Z(M_Z)}{M_Z^2} + \text{vertex} + \text{box} . \quad (10)$$

Equation (9) includes the light quark contribution extracted from experimental data,⁴ together with the leptonic contribution. It also contains the logarithms of the W -boson, top-quark, charged-Higgs, squark, slepton, and chargino masses. In eq. (10), the $\hat{\Pi}$ denote the real and transverse parts of the gauge boson self-energies, evaluated in the \overline{DR} scheme. Equation (10) also includes the vertex and box contributions that renormalize the Fermi constant, as well as the leading higher-order m_t^4 and QCD standard-model corrections given in ref. 5. (For more details about our calculation see [6].)

From these results we find the weak gauge couplings $\hat{g}_1(M_Z)$ and $\hat{g}_2(M_Z)$ using the \overline{DR} relations

$$\hat{g}_1(M_Z) = \sqrt{\frac{5}{3}} \frac{\hat{e}}{\hat{s}} , \quad \hat{g}_2(M_Z) = \frac{\hat{e}}{\hat{s}} , \quad (11)$$

where $\hat{\alpha} = \hat{e}^2/4\pi$. These couplings serve as the weak-scale boundary conditions for the two-loop supersymmetric RGE's.⁷ Note that they depend on the masses of the supersymmetric particles, which are determined self-consistently through the solution to the renormalization group equations. The \overline{DR} values for $\hat{g}_1(M_Z)$ and $\hat{g}_2(M_Z)$ contain the full one-loop threshold corrections, including the logarithmic and finite contributions.

2.3. Mass Thresholds

Since the exact one-loop self-energies have been computed for all particles in the minimal supersymmetric standard model,⁸ it is possible to include all the logarithmic and finite corrections in the threshold corrections. In this section we will discuss the leading corrections for the top- and bottom-quark masses.

The relation between the top-quark pole mass and the running \overline{DR} mass is given by

$$m_t = \hat{m}_t(\mu) - \hat{\Sigma}_t(m_t) , \quad (12)$$

where \hat{m}_t is the \overline{DR} mass, and $\hat{\Sigma}_t$ is the top-quark self-energy, defined by $\hat{\Sigma}_t = \hat{\Sigma}_1 + m_t \hat{\Sigma}_\gamma$, and the quark self-energy is written $\hat{\Sigma}_1 + \hat{\Sigma}_\gamma \not{p} + \hat{\Sigma}_{\gamma 5} \not{p} \gamma_5 + \hat{\Sigma}_5 \gamma_5$.

Equation (12) relates the running mass to the pole mass at *any* scale μ near m_t . In a unification analysis, this leads to a computational simplification because the RGE's can be run down to a single scale μ , and then all the threshold corrections applied simultaneously. For the case at hand, we take the scale $\mu = M_Z$.

The top quark threshold correction receives its most important contributions from gluon and gluino/squark loops. The correction from the gluon loop is well-known,^{*}

$$m_t = \hat{m}_t(\mu) \left\{ 1 + \frac{\alpha_s}{3\pi} \left[5 + 6 \log \left(\frac{\mu}{m_t} \right) \right] \right\} , \quad (13)$$

^{*}Actually this correction is more commonly seen as $4\alpha_s/(3\pi)$, which is the result for $\mu = m_t$ in the \overline{MS} scheme.

where $\hat{m}_t(\mu)$ is the running \overline{DR} mass evaluated at the scale μ . For $\mu = m_t$, this correction is about 6%. The gluino/squark contribution is given by

$$\begin{aligned} \Delta m_t^{\tilde{g}\tilde{q}} = & -\frac{\alpha_s}{3\pi} \left\{ \text{Re} \left[B_1(m_t, m_{\tilde{g}}, m_{\tilde{t}_1}) + B_1(m_t, m_{\tilde{g}}, m_{\tilde{t}_2}) \right] \right. \\ & \left. - \frac{2m_{\tilde{g}}(A_t + \bar{\mu} \cot \beta)}{m_{\tilde{t}_1}^2 - m_{\tilde{t}_2}^2} \text{Re} \left[B_0(m_t, m_{\tilde{g}}, m_{\tilde{t}_1}) - B_0(m_t, m_{\tilde{g}}, m_{\tilde{t}_2}) \right] \right\} \hat{m}_t(\mu) , \end{aligned} \quad (14)$$

where B_0 and B_1 are the two point functions

$$B_n(p, m_1, m_2) = - \int_0^1 dx x^n \log \left(\frac{(1-x)m_1^2 + x m_2^2 - x(1-x)p^2}{\mu^2} \right) , \quad (15)$$

and $\bar{\mu}$ is the Higgs mass parameter. This expression contains a finite plus a logarithmic piece for $m_{\tilde{g}} > m_t$ and/or $m_{\tilde{t}} > m_t$. The logarithmic contribution, which can be larger than the gluon contribution (13), is given correctly by the match-and-run procedure. The finite piece is of order 1%.

The bottom-quark mass also receives a significant threshold correction, similar to (13), from the diagram with a gluon loop. For $\mu = M_Z$, the large logarithm $\log(m_b/M_Z)$ must be resummed to determine the pole mass. For the bottom quark, the correction from the gluino/squark diagram is also important; the second line in (14) becomes

$$\frac{\Delta m_b}{m_b} \simeq -\frac{2\alpha_s}{3\pi} \frac{\bar{\mu} m_{\tilde{g}}}{m_{\tilde{b}}^2} \tan \beta \quad (16)$$

for large $\tan \beta$. This correction,⁹ which is completely missed in the match-and-run procedure, can be as large as 50%. In the following, we choose $\bar{\mu} > 0$ to minimize the bottom-quark mass.

2.4. Yukawa Coupling Thresholds

To discuss supersymmetric unification, and in particular, bottom-tau Yukawa coupling unification, one needs to find the running \overline{DR} Yukawa couplings. In this section we will show how to use the mass threshold corrections to find the running \overline{DR} Yukawa couplings. The \overline{DR} Yukawa couplings contain all the weak-scale threshold corrections.

Let us illustrate our procedure for the case of the top quark. As above, we find the running \overline{DR} mass from the physical pole mass using (12). We then relate the \overline{DR} mass to the \overline{DR} vev and Yukawa coupling by the simple relation

$$\hat{m}_t(\mu) = \frac{1}{\sqrt{2}} \hat{\lambda}_t(\mu) \hat{v}_2(\mu) . \quad (17)$$

The \overline{DR} vev is determined from the gauge couplings and the Z -boson mass,

$$M_Z^2 = \frac{1}{4} (\hat{g}(\mu)^2 + \hat{g}'(\mu)^2) \hat{v}^2 - \hat{\Pi}_Z(M_Z) . \quad (18)$$

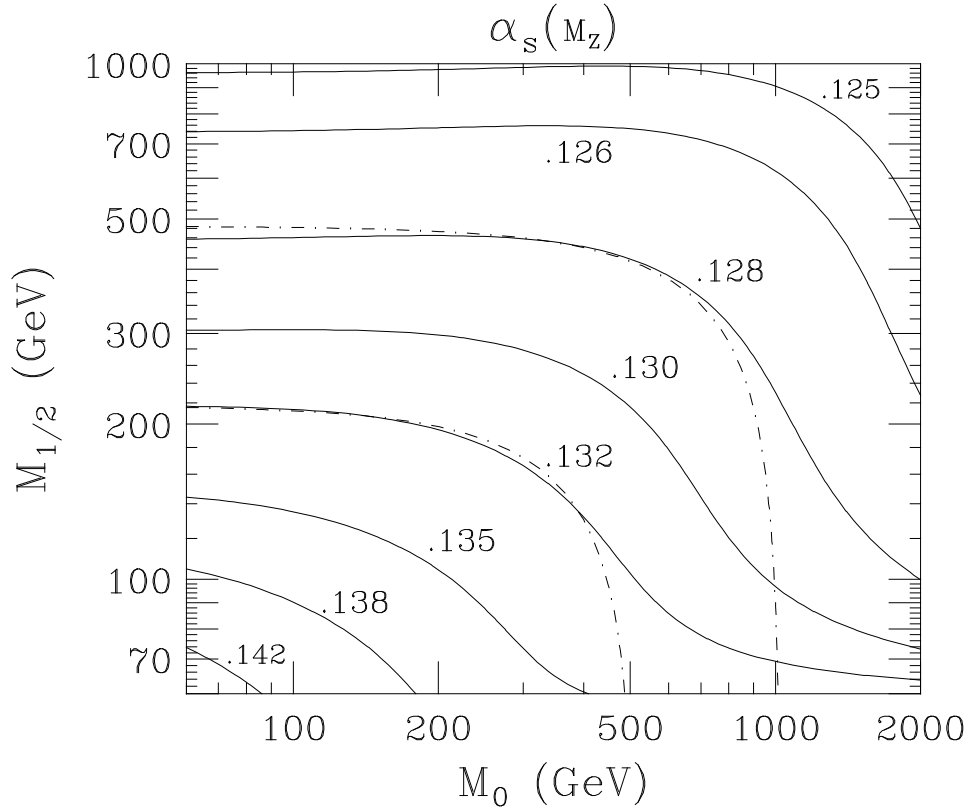


Fig. 3. Contours of $\alpha_s(M_Z)$ and one-loop light-squark masses in the $M_0, M_{1/2}$ plane, with $m_t = 170$ GeV, $\tan\beta = 2$ and $A_0 = 0$. The dot-dashed contours indicate squark masses of 500 and 1000 GeV. The squark masses obey the heuristic relation $m_q^2 \simeq M_0^2 + 4.5 M_{1/2}^2$.

Combining these expressions, we find the threshold-corrected Yukawa coupling,

$$\hat{\lambda}_t(\mu) = \frac{\hat{g}_2(M_Z)}{\sqrt{2}\hat{c}} \frac{m_t}{M_Z} \left[1 + \frac{\hat{\Sigma}_t(m_t)}{m_t} - \frac{1}{2} \frac{\hat{\Pi}_Z(M_Z)}{M_Z^2} \right], \quad (19)$$

where m_t is the top-quark pole mass. Equation (19) converts the measured top-quark mass into a threshold-corrected Yukawa coupling at the scale μ .

Following this procedure, we can find all the threshold-corrected Yukawa couplings in terms of two-point functions. The great advantage of this approach is that the final formulae are much simpler than those obtained using three-point diagrams.

3. Numerical Analysis

3.1. Gauge Coupling Unification

Now that we have the full set of one-loop threshold corrections, we can carry out a consistent numerical evaluation of the two-loop supersymmetric RGE's. In what follows we will study correlations between the low-energy supersymmetric spectrum and the physics of the unification scale.

As a point of reference, we show in Figure 3 our results for $\alpha_s(M_Z)$ in the $M_0, M_{1/2}$ plane, with no unification-scale threshold corrections, for $m_t = 170$ GeV, $\tan\beta = 2$,

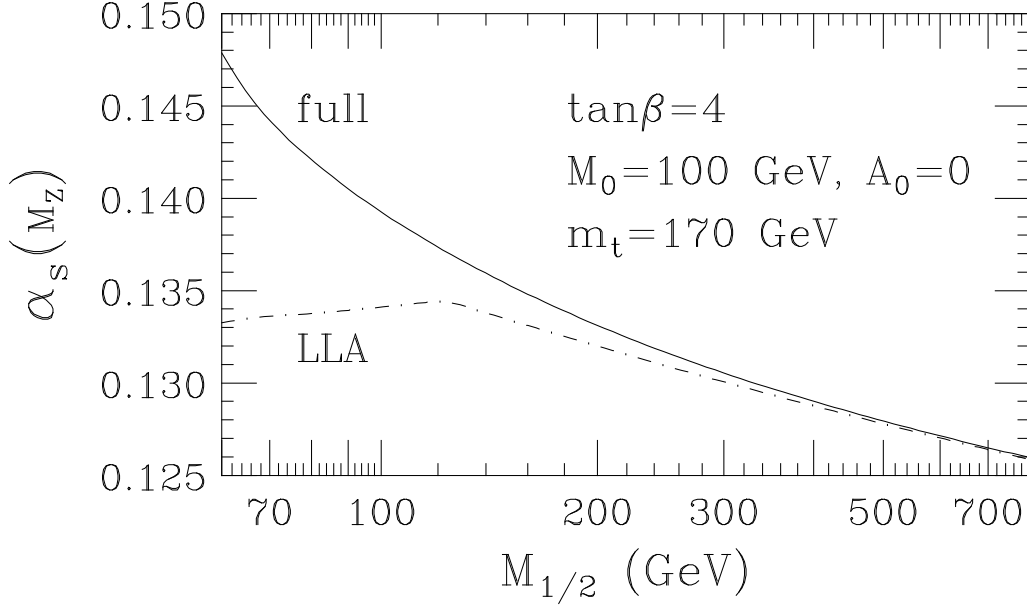


Fig. 4. The \overline{MS} coupling $\alpha_s(M_Z)$ vs. $M_{1/2}$. The curve labeled LLA shows the result if we include only the logarithms of the supersymmetric masses (the leading logarithm approximation), while the solid line corresponds to the full result including all finite corrections.

and $A_0 = 0$. Comparing with the value from the particle data group,¹⁰ $\alpha_s(M_Z) = 0.117 \pm 0.005$, we see that $\alpha_s(M_Z)$ is rather large.

The value of $\alpha_s(M_Z)$ is correlated with the low-energy supersymmetric spectrum through its dependence on M_0 and $M_{1/2}$. In Figure 3 we also show representative values of the light-squark masses in the $M_0, M_{1/2}$ plane. If, for naturalness, we require the squark masses to be below 1 TeV, we find the lower bound $\alpha_s(M_Z) > 0.127$ from Figure 3.

The values of $\alpha_s(M_Z)$ quoted here are larger than in many previous analyses for two reasons. First, during the past few years, the best-fit value for the top-quark mass has been increasing. This implies a decreasing central value for the standard-model weak mixing angle, which then leads to an increase in $\alpha_s(M_Z)$. Second, the finite corrections decrease \hat{s}^2 , which leads to a further increase in $\alpha_s(M_Z)$. The finite corrections are important in the region $M_{1/2} \lesssim 200$ GeV where $\alpha_s(M_Z)$ is appreciably larger than in the leading logarithmic approximation, as shown in Figure 4.

Of course, the value of $\alpha_s(M_Z)$ can be reduced by a unification-scale threshold correction with $\epsilon_g < 0$. This is illustrated in Figure 5, where we show the upper and lower bounds on ϵ_g necessary to obtain $\alpha_s(M_Z) = 0.117 \pm 0.01$. We find that ϵ_g of just -2% is sufficient for a wide range of supersymmetric masses. For squark masses of order 1 TeV, no unification thresholds are required.

3.2. Yukawa Coupling Unification

In typical SU(5) models, the bottom and tau Yukawa couplings unify at the scale M_{GUT} . This leads to a prediction for the bottom-quark pole mass, m_b , as a function of

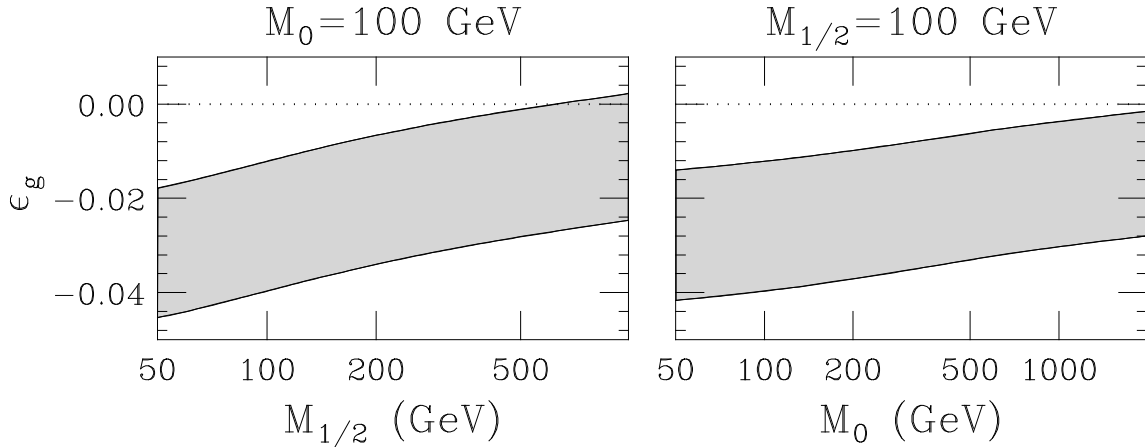


Fig. 5. The shaded regions indicate the allowed values of the gauge coupling threshold correction, ϵ_g , necessary to obtain $\alpha_s(M_Z) = 0.117 \pm 0.01$, with $m_t = 170$ GeV, $\tan\beta = 2$ and $A = 0$.

m_t and $\tan\beta$. For $m_t \simeq 170$ GeV and arbitrary $\tan\beta$, one typically finds a bottom-quark mass above the range experiment,¹⁰ which we take to be $4.7 < m_b < 5.2$ GeV. There are two regions of $\tan\beta$ where m_b is smaller and successful bottom-tau unification is easier to achieve: $\tan\beta \lesssim 2$ and $\tan\beta \gtrsim 40$.

In the region $\tan\beta \lesssim 2$, the top-quark Yukawa coupling is large, approaching the perturbative limit. The large coupling drives electroweak symmetry breaking and significantly affects the RGE for the bottom-quark Yukawa. It pushes $\hat{\lambda}_b(M_Z)$ down and decreases the bottom-quark mass. In the region of large $\tan\beta$, both the top- and bottom-quark Yukawa couplings are large. They both make significant contributions to the RGE's. Indeed, for large $\tan\beta$, the large bottom-quark Yukawa actually drives *down* the value of the bottom-quark mass. Therefore we have the possibility of successful bottom-tau unification for small and large $\tan\beta$.

In Figure 6 we show m_b and $\alpha_s(M_Z)$ versus m_t , for small $\tan\beta$ and various values of M_0 , and $M_{1/2}$, with no unification-scale thresholds. The figure corresponds to $\hat{\lambda}_t(M_{\text{GUT}}) = 3$. Smaller values of $\hat{\lambda}_t(M_{\text{GUT}})$ give rise to larger values of m_b , so the curves can be interpreted as lower limits on the bottom-quark mass (in the small $\tan\beta$ region). We see that m_b is large unless the squark masses are of order 1 TeV.

In Figure 7 we show m_b and $\alpha_s(M_Z)$ versus $\tan\beta$, in the large $\tan\beta$ region, for $m_t = 170$, and various values of M_0 , and $M_{1/2}$, with no unification-scale thresholds. For each point, we choose the maximum value of $\tan\beta$ subject to the physical requirements $m_A > 22$ GeV, $m_{\tilde{\tau}} > 45$ GeV and $m_{\chi_1^+} > 47$ GeV, where A is the CP-odd Higgs boson, $\tilde{\tau}$ is the tau slepton, and χ_1^+ is the lightest chargino. From the figure we see that the smallest values of m_b occur for squark masses near 1 TeV.

As with $\alpha_s(M_Z)$, the picture is changed by unification-scale threshold corrections. To understand their effects, note the striking similarity between the m_b and $\alpha_s(M_Z)$ curves in Figures 6 and 7. This tells us that the value of m_b is tightly correlated with the value of $\alpha_s(M_Z)$. It leads us to expect that the gauge threshold correction will have an important effect on m_b .

This expectation is confirmed in Figure 8, where we show the band of unification-

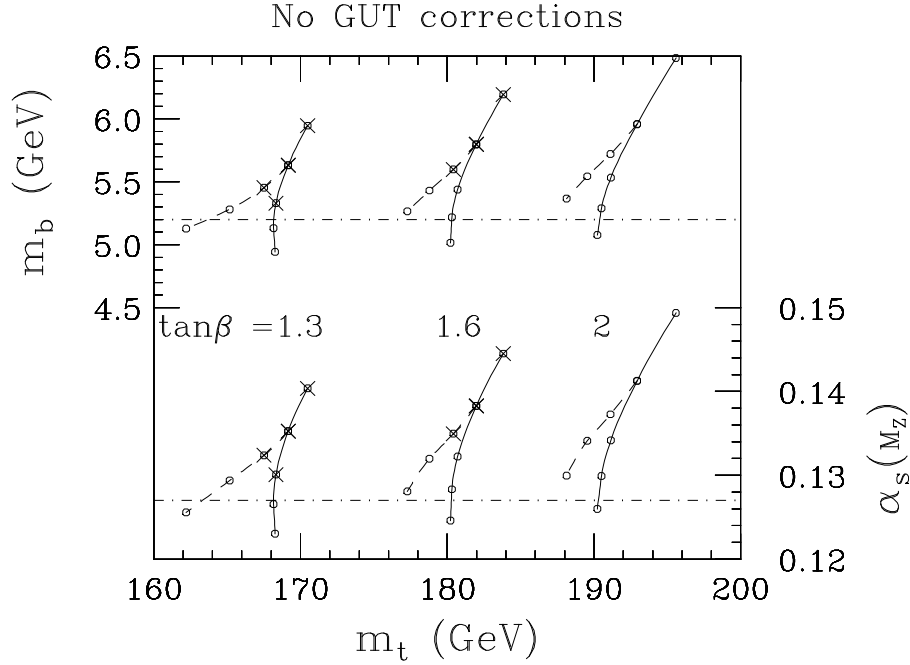


Fig. 6. The bottom-quark pole mass and $\alpha_s(M_Z)$ vs. m_t , with no unification-scale thresholds, for various values of $\tan\beta$, for $A_0 = 0$ and $\hat{\lambda}_t(M_{\text{GUT}}) = 3$. The right (solid) leg in each pair of lines corresponds to $M_{1/2}$ varying from 60 to 1000 GeV, with M_0 fixed at 60 GeV. The left (dashed) leg corresponds to M_0 varying from 60 to 1000 GeV, with $M_{1/2} = 100$ GeV. On the solid lines the circles mark, from top to bottom, $M_{1/2} = 60, 100, 200, 400$, and 1000 GeV, and on the dashed lines the circles mark $M_0 = 60, 200, 400$, and 1000 GeV. The lowest point on each left leg and the second-to-lowest point on each right leg corresponds to $m_{\tilde{q}} \simeq 1$ TeV. The \times 's mark points with one-loop Higgs mass $m_h < 60$ GeV.

scale thresholds ϵ_b that are necessary to bring m_b into the preferred range. For the figure, we first choose ϵ_g to fix $\alpha_s(M_Z)$ at its central value, $\alpha_s(M_Z) = 0.117$. We then vary ϵ_b to obtain $4.7 < m_b < 5.2$. The two bands of ϵ_b correspond to the regions of small and large $\tan\beta$. In the first region, we set $\tan\beta = 2.5$, and in the second, $\tan\beta = 30$. The figure indicates that Yukawa threshold corrections of less than 10% are sufficient to ensure successful unification, provided the gauge thresholds are such that $\alpha_s(M_Z)$ agrees with experiment.

4. Conclusions

In this talk we discussed the complete one-loop weak-scale threshold corrections in the minimal supersymmetric standard model. We illustrated how they affect gauge and Yukawa unification, with and without unification-scale threshold corrections. In the absence of such corrections, we find that $\alpha_s(M_Z)$ and m_b are large unless the squark masses are of order one TeV. With small threshold corrections, we find acceptable values for $\alpha_s(M_Z)$ and m_b for heavy or light supersymmetric spectra.

We would like to thank R. Zhang for collaboration during the early stages of this work, and S. Pokorski for helpful discussions. J.B. would like to thank Z. Pluciennik for extensive discussions during the conference. This work was supported by the U.S.

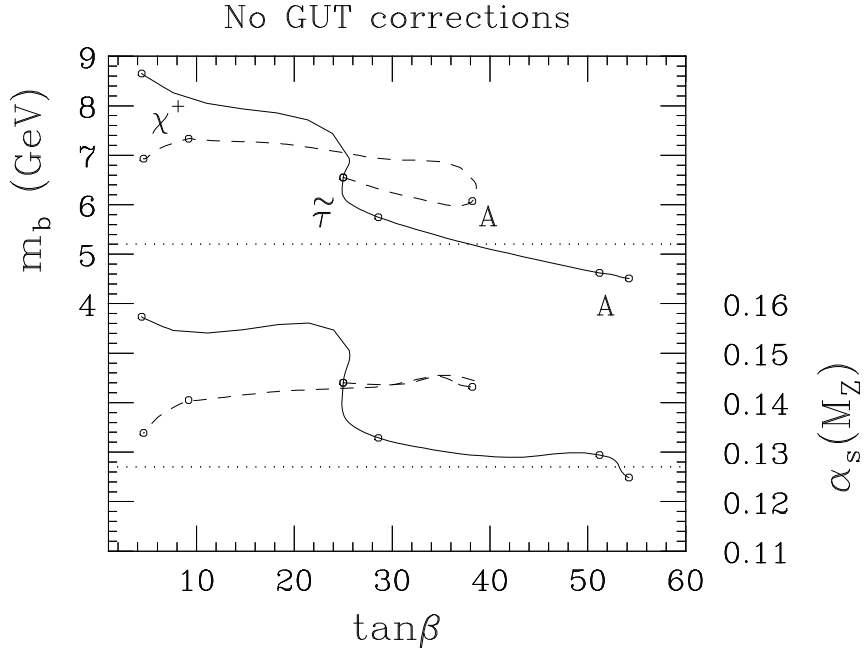


Fig. 7. The bottom-quark pole mass and $\alpha_s(M_Z)$ vs. the maximum $\tan\beta$, with no unification-scale thresholds, for $m_t = 170$ GeV and $A_0 = 0$. The solid line corresponds to $M_{1/2}$ varying from 60 to 1000 GeV, with M_0 fixed at 60 GeV. The dashed line corresponds to M_0 varying from 60 to 1000 GeV, with $M_{1/2} = 100$ GeV. On the solid lines the circles mark, from top to bottom, $M_{1/2} = 60, 100, 200, 400$, and 1000 GeV, and on the dashed lines the circles mark $M_0 = 60, 200, 400$, and 1000 GeV. The maximum value of $\tan\beta$ is determined by the experimental limits on the masses of the A , $\tilde{\tau}$ and the χ_1^+ , as indicated.

National Science Foundation under grant NSF-PHY-9404057.

5. References

1. H. Georgi, H.R. Quinn and S. Weinberg, *Phys. Rev. Lett.* **33** (1974) 451;
S. Dimopoulos, S. Raby and F. Wilczek, *Phys. Rev.* **D24** (1981) 1681;
L. Ibanez and G. Ross, *Phys. Lett.* **B105** (1981) 439;
U. Amaldi, A. Bohm, L. Durkin, P. Langacker, A. Mann, W. Marciano, A. Sirlin and H. Williams, *Phys. Rev.* **D36** (1987) 1385;
J. Ellis, S. Kelley and D. Nanopoulos, *Phys. Lett.* **B249** (1991) 441; **B260** (1991) 131;
P. Langacker and M. Luo, *Phys. Rev.* **D44** (1991) 817;
U. Amaldi, W. de Boer and H. Furstenau, *Phys. Lett.* **B260** (1991) 447;
F. Anslemo, L. Cifarelli, A. Peterman and A. Zichichi, *Nuovo Cimento* **104A** (1991) 1817.
2. P. Chankowski, Z. Pluciennik and S. Pokorski, Warsaw preprint IFT-94/19. See also the contributions of these authors to these proceedings.
3. G. Degrassi, S. Fanchiotti and A. Sirlin, *Nucl. Phys.* **B351** (1991) 49, and references therein.

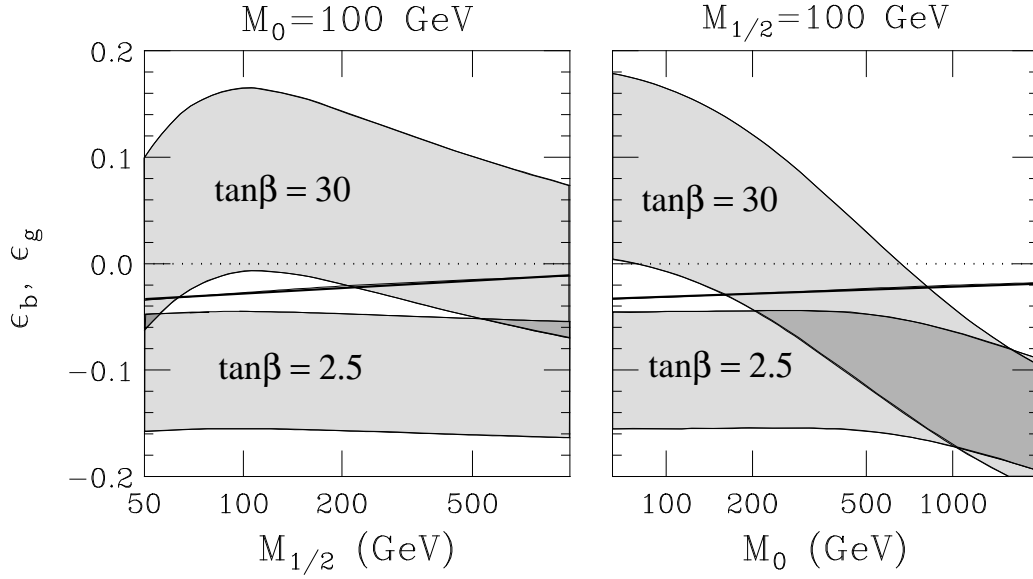


Fig. 8. Values of the bottom-quark Yukawa coupling threshold correction, ϵ_b , necessary to obtain $4.7 < m_b < 5.2$, assuming ϵ_g is adjusted to give $\alpha_s(M_Z) = 0.117$. The solid line marks ϵ_g , while the two bands indicate ϵ_b for different values of $\tan\beta$, for $A_0 = 0$ and $m_t = 180$ GeV.

4. We use the result of the most recent analysis of Jegerlehner as quoted in B.A. Kniehl, preprint KEK-TH-412 (1994).
5. S. Fanchiotti, B. Kniehl and A. Sirlin, *Phys. Rev.* **D48** (1993) 307.
6. J. Bagger, K. Matchev, D. Pierce and R. Zhang, to appear.
7. M.E. Machacek and M.T. Vaughn, *Nucl. Phys.* **B222** (1983) 83; *ibid.* **B236** (1984) 221; *ibid.* **B249** (1985) 70;
I. Jack, *Phys. Lett.* **B147** (1984) 405;
S. Martin, M. Vaughn, Northeastern preprint NUB-3081-93-TH (1993);
Y. Yamada, *Phys. Rev.* **D50** (1994) 3537.
8. The MSSM gauge and Higgs sector self energies can be found in P.H. Chankowski, S. Pokorski and J. Rosiek, *Nucl. Phys.* **B423** (1994) 437.
The gaugino/Higgsino mass corrections are in D. Pierce and A. Papadopoulos, *Phys. Rev.* **D50** (1994) 565; *Nucl. Phys.* **B430** (1994) 278.
The threshold functions for the entire MSSM spectrum are in ref. 6.
9. L.J. Hall, R. Rattazzi and U. Sarid, *Phys. Rev.* **D50** (1994) 7048;
M. Carena, M. Olechowski, S. Pokorski and C.E.M. Wagner, *Nucl. Phys.* **B426** (1994) 269;
R. Hempfling, *Z. Phys.* **C63** (1994) 309.
10. Particle Data Group Review of Particle Properties, *Phys. Rev.* **D50** (1994) 1.